Rydberg spectroscopy of single-electron capture in low-energy collisions of Ar^{9+} and Ar^{8+} with cesium

S. Martin and A. Denis
Laboratoire de Spectrométrie Ionique et Moléculaire, Université Lyon 1, 43 boulevard du 11 Novembre 1918, 69622 Villeurbanne CEDEX, France

Y. Ouerdane
Laboratoire de Traitement du Signal et Instrumentation, Faculté des Sciences et Techniques, 23 rue du Dr. Paul Michelon, 42023 St. Etienne, CEDEX 02, France

M. Carré, M. C. Buchet-Poulizac, and J. Désesquelles
Laboratoire de Spectrométrie Ionique et Moléculaire, Université Lyon 1, 43 boulevard du 11 Novembre 1918, 69622 Villeurbanne CEDEX, France
(Received 7 February 1992)

Optical spectroscopy has been used to study electron capture into Ar^{9+} and Ar^{8+} ions from cesium at several impact energies of between 8 and 180 keV. Many Rydberg lines were observed. At high spectral resolution the quasi-l-degeneracy of final Rydberg states was removed and the fine-structure components of doubly excited Rydberg transitions were resolved. Cross sections for state-selective electron capture in collision of Ar^{8+} with cesium were determined and then compared with theoretical data calculated by means of a three-body classical-trajectory Monte Carlo method and with predictions of a classical barrier model.

PACS number(s): 34.70.+e, 34.50.Fa, 32.30.Jc

I. INTRODUCTION

Electron capture into excited states is a very important process in collisions between multicharged ions and atoms since the associated cross sections are large, particularly in the domain of low and intermediate energies. Knowledge about the process of charge exchange is crucial for a better understanding of atomic collisions in general and for their applications to high-temperature plasmas.

The electron-capture process in collisions of multiply charged ions with atoms is a field of various experimental and theoretical investigations. After early works on determination of the total cross sections in atomic and molecular hydrogen and in other neutral atoms, interest has proceeded to the detailed analysis of product-state distributions showing the selective population into excited states, the importance of multiple-electron-capture processes, and the role of the autoionization and stabilization of electrons in the projectile. The complexity of a theoretical approach to the problems by means of quantum-mechanical or semiclassical methods is clearly shown by the recent report of Harel and Salin [1] on the mechanisms governing the final n,l,m state distributions of the captured electron in slow collisions between multicharged ions and atomic hydrogen. However, when the electron is captured into high-lying states, the process is expected to be well described by classical models such as the three-body classical-trajectory Monte Carlo [2] and the over-barrier methods. The preferential final states and the cross sections can then be predicted. Very simple formulas of single-electron capture are obtained by the over-barrier model of Ryufuku and Watanabe [3]. The distance at which capture takes place dominantly can be approximated by the formula $R=(1+2\sqrt{q})/I$, where q is the charge of the incident ion and I is the binding energy of the electron in its initial state. From the resonant energy condition at R distance, $E=I+q/R$, the value of the principal quantum number of the most populated state is deduced to be $n\simeq\sqrt{(1+2\sqrt{q})/2I(q+2\sqrt{q})}$. In previous works [4,5] using uv spectroscopy, we found that, in collisions of Ar^{9+} and Ar^{8+} with H_2 and rare-gas atoms, the electron is captured in low-lying states $n=4$ and 5. However, in collisions with alkali-metal atoms the outer electron is very loosely bound so that the capture in Rydberg states can be expected. In cesium, the 6s electron is bound by 3.9 eV only, the capture distance R is large ($R=24$ Å for Ar^{8+}-Cs), and consequently the excitation cross section is also very large ($\sigma\simeq 9\times 10^{-14}$ cm^2) and the dominantly populated states are high ($n=10$ and 11). Furthermore, when the binding energy of the electron in its initial state is so low, two electrons could easily be captured by a multiply charged ion, either directly in a double-electron-capture collision with an alkali-metal atom, or in two successive collisions. We observed both of these processes in previous works [6,7].

In this paper we present results of our analysis of optical spectra emitted in the visible spectral range by Ar^{8+} and Ar^{7+} ions excited into singly and doubly excited Rydberg states after collisions of Ar^{9+} and Ar^{8+} projectiles with cesium atoms. l sublevels of singly excited Rydberg transitions were resolved using high-resolution

spectroscopy. j-sublevel degeneracy of doubly excited Rydberg transitions was partially lifted. Emission cross sections of Rydberg transitions were measured at various energies. n distributions of the captured electron were deduced from the measured emission cross sections by taking the cascades into account. Results of state distributions and absolute cross sections are compared to theoretical predictions of the extended classical barrier model (ECBM) of Niehaus [8] and the three-body classical-trajectory Monte Carlo (CTMC) model of Pascale, Olson, and Reinhold [9].

II. EXPERIMENT

Our measurements are based on the observation of visible photons emitted by primary ions as a result of electron capture from cesium atoms.

The experimental arrangement used in the present work has been described previously. It is briefly outlined here. A beam of Ar^{q+} ($q=8$ or 9), extracted through potentials between 1 and 20 kV from the electron cyclotron resonance (ECR) ion source of the LAGRIPPA facility, is mass and charge analyzed by means of two successive magnets, and passed through a cesium vapor produced in a heated cell. A temperature variation between 30 and 90 °C corresponds to a range of cesium vapor pressure of 6×10^{-6}–3×10^{-4} mbar. The photons resulting from Ar^{q+}-Cs collisions were observed perpendicular to the ion beam direction, diffracted by a 0.6-m Czerny-Turner spectrometer equipped with either a 1200-line/mm grating blazed at 300 nm or a 3600-line/mm holographic grating blazed at 270 nm and finally detected by a 6256 S EMI photomultiplier cooled down to −20 °C. Under normal observation conditions, the spectrometer aperture was maximum (±5°); the resolution was then limited by the Doppler broadening ($\Delta\lambda/\lambda=2.6\times10^{-4}$ at 180-keV energy at which argon ion velocity is $\beta=3.1\times10^{-3}$). By considerably reducing the aperture and using a 3600-line/mm grating we obtained a spectral resolution of 0.02 nm [full width at half maximum (FWHM)]. Spectra were recorded in the wavelength range 200–500 nm.

Two different incident Ar^{8+} beams were successively passed through the cesium target. One was the Ar^{8+} beam directly issued from the ECR source. The other was "prepared" from the Ar^{9+} beam produced by the ion source, by means of electron-capture collisions in a nitrogen cell set between the two magnetic analyzers of the beam line. The electron capture collisions result in an outgoing "prepared" Ar^{8+} beam which has a high metastable fraction in it (about 30%).

III. RESULTS

A. Spectra

Typical low-resolution spectra obtained at a low pressure of the cesium vapor ($T\simeq50$ °C) with Ar^{9+}, "primary" Ar^{8+} and "prepared" Ar^{8+} beams are displayed in Fig. 1 together with an identification of the strongest lines. These spectra present unresolved lines the wavelengths of which are approximately equal to hydrogenic

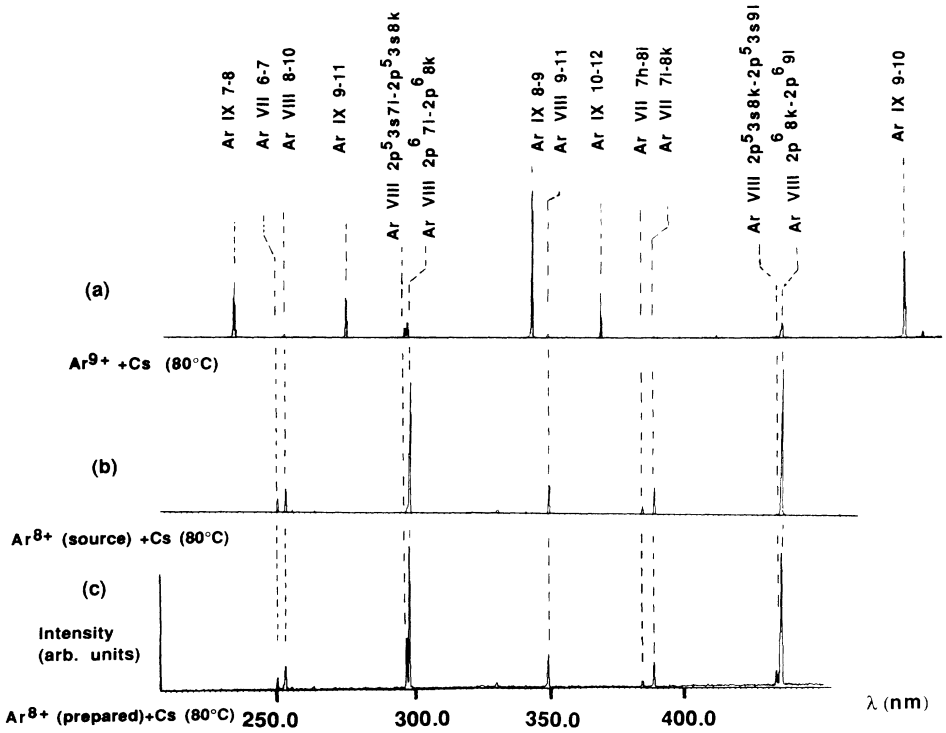

FIG. 1. Spectra observed from 200 to 500 nm after the collision in cesium at 80 °C of (a) Ar^{9+}, (b) Ar^{8+} (directly from the ion source), (c) Ar^{8+} (prepared by electron capture from an Ar^{9+} primary beam). Lines assigned to Ar VII, Ar VIII, and Ar IX refer to Rydberg transitions.

values. They are assigned to $\Delta n=1$, 2, and 3 ($n=7-11$) transitions in Ar VII, VIII, and IX. At wavelengths just lower than the Ar VIII $7i$-$8k$ and $8k$-$9l$ lines, doubly excited Rydberg transitions were observed. These transitions are more intense when an incident beam of Ar^{8+} was "prepared" proving that the doubly excited states $3s$ $9l$ and $3s$ $8k$ of Ar VIII are produced by one-electron capture into the metastable $1s^22s^22p^53s\ ^3P_{0,2}$ Ar^{8+} ions which are much more populated in a "prepared" beam (about 30%) than in a "primary" beam (a few percent). This observation demonstrates that the interpretation given in a previous paper [6] about the production of these doubly excited states was right. They are produced either by single-electron capture into Ar^{8+} prepared into a metastable state or by double collision into Ar^{9+}.

High-resolution spectra were recorded with Ar^{8+} and Ar^{9+} incident beams. An example of resolution obtained is shown in Fig. 2 which displays $2p^6(nl)$-$2p^6(n+1,l+1)$ and $2p^53s(nl)$-$2p^53s(n+1,l+1)$ transitions in Ar VIII emitted after double collisions of Ar^{9+} ions in cesium with a 0.02-nm FWHM. Wavelengths of Ar VIII lines produced by Ar-Cs collisions and measured between 200 and 500 nm are reported in Table I together with computed hydrogenic values for $\Delta n=1$, 2, and 3 transitions. As the difference between the wavelengths of j components of $(n,l=n-1)$-$(n+1,l'=n)$ transitions between singly excited states calculated using a multiconfiguration

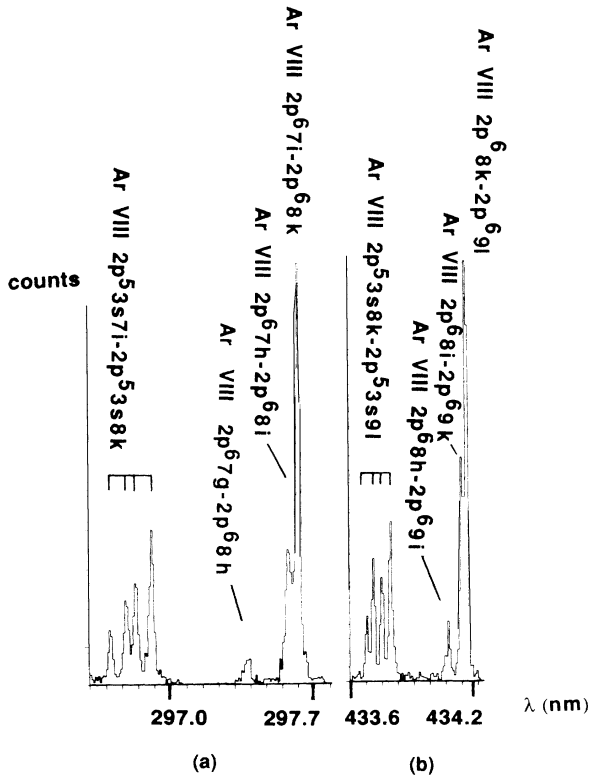

FIG. 2. High-resolution spectra of Ar VIII following simple electron capture by Ar^{8+} from a cesium target, and showing the fine-structure splitting of core excited multiplets Ar *VIII* (a) $2p^53s7i$-$2p^53s8k$ and (b) $2p^53s8k$-$2p^53s9l$ and the energy separations of transitions between singly excited levels (a) $2p^6$ $7i$-$8k$, $7h$-$8i$, $7g$-$8h$, and (b) $2p^6$ $8k$-$9l$, $8i$-$9k$, $8h$-$9i$.

TABLE I. Rydberg transitions of Ar VIII observed after collisions of Ar^{9+} on Cs (90°C). Doubly excited states are produced by double collisions. $1s^22s^22p^53s$ core configuration is marked by an asterisk.

Identification	λ measured (nm)	λ hydrogenic (nm)
$8k$-$10l$*	252.92	
	252.96	
$8h$-$10i$	253.09	
$8i$-$10k$	253.12	253.13
$8k$-$10l$	253.12	253.13
$9l$-$12m$	263.62	263.62
$7i$-$8k$*	296.68	
	296.77	
	296.81	
	296.90	
$7g$-$8h$	297.39	
$7h$-$8i$	297.61	
$7i$-$8k$	297.66	297.68
$9l$-$11m$*	348.55	
$9k$-$11l$	348.88	348.88
$9l$-$11m$	348.88	348.88
$8k$-$9l$*	433.65	
	433.68	
	433.73	
	433.77	
$8h$-$9i$	434.09	
$8i$-$9k$	434.16	
$8k$-$9l$	434.18	434.19
$10l$-$12m$	465.99	465.99
$10m$-$12n$	465.99	465.99

Dirac-Fock (MCDF) code [10] proved to be negligible (0.008 nm for $7i$-$8k$), it appears that the structure observed in Fig. 2, at wavelengths quoted in Table I, is due to l-sublevel splitting. The shifts observed between l components $(n,l=n-x)\rightarrow(n+1,l'=n-x+1)$, for example, $7i$-$8k$, $7h$-$8i$, $7g$-$8h$, are due to long-range forces. As the penetration calculated with a MCDF code is found to be negligible, an effective value for the dipole polarizability of the $1s^22s^22p^63s$ core can be deduced from the measured shifts using hydrogenic values for $\langle r^{-4}\rangle$. The result $\alpha=(0.035\pm0.01)a_0^3$ is in fair agreement with a rough estimate of the ground-state electric dipole polarizability $\alpha'=0.025a_0^3$ deduced from the theoretical energies and lifetimes of Bureeva and Safronova [11] which took only the 3-2 transitions into account. Our measurement is also consistent with the polarizability of isoelectronic Na-like chlorine, α(Cl VIII) $=0.0434a_0^3$ [12], deduced from beam foil measurements [13]. Quadrupole polarizabilities and dynamical contributions, depending on $\langle r^{-6}\rangle$, are very low and these components of polarization are negligible for high quantum number levels. In doubly excited states $2p^53snl$, the fine structure is partly resolved but comparison with theories is much more complicated.

B. Cross sections

Cross sections for emission of Ar VIII lines after Ar^{8+}-Cs collisions were determined at five energies be-

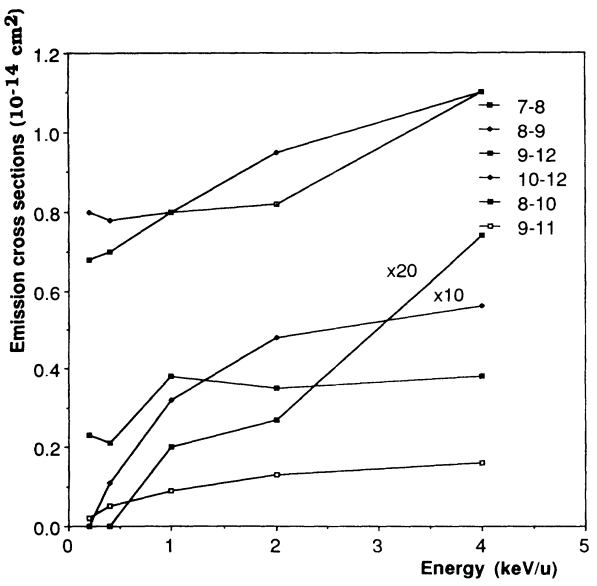

FIG. 3. Cross sections for the emission of singly excited Ar VIII Rydberg lines in $Ar^{8+}+Cs$ collisions from 0.2 to 4 keV/u.

tween 8 and 160 keV (Fig. 3). They were deduced from the measured line intensities and the target density calculated from the temperature of the cesium oven. The absolute response of the optical system was determined at wavelengths 302.89 and 306.91 nm of Ar VIII $5p\ ^2P_{1/2}-5d\ ^2D_{3/2}$ and $5p\ ^2P_{3/2}-5d\ ^2D_{5/2}$ transitions, respectively, using emission cross sections of these lines after $Ar^{8+}+H_2$ collisions calculated from the known cross sections of Ar VIII 3*p*-5*d* [14] and branching ratios [15]. Absolute values for emission cross sections were deduced in the whole spectral range by combining the absolute calibration at these two wavelengths and the spectral response of the detection system. All emission cross sections are believed to be accurate within a factor of 2 or 3. Relative accuracy is at least within 20%. Results for emission cross sections of 7-8, 8-9, 8-10, 9-11, 9-12, and 10-12 transitions in Ar VIII are displayed in Table II. At 8 keV, ion beam intensities are too low to obtain a good determination of cross sections for resolved structures. Results given were deduced from the total intensities of unresolved peaks. Emission cross sections of Rydberg transitions summed on l levels were determined within the energy range 0.2–4 keV/u (Fig. 3). Variations are smooth for 7-8 and 8-9 transitions and sharp for 9-12 and 10-12 transitions for which there is a drastic decrease at low energies showing that observed n distribution depends significantly on collision velocity.

TABLE II. Emission cross section of Ar VIII transitions in collision of Ar^{8+} on Cs at impact energies of 8 and 160 keV.

	$\sigma_{emission}$ (10^{-14} cm^2)	
Identification	160 keV	8 keV
8*h*-10*i*	0.09	
8*i*-10*k* plus 8*k*-10*l*	0.29	
Total 8-10	0.38	0.23
9*k*-12*l* plus 9*l*-12*m*	0.04	0.00
7*g*-8*h*	0.05	
7*h*-8*i*	0.28	
7*i*-8*k*	0.76	
Total 7-8	1.09	0.70
9*k*-11*l* plus 9*l*-11*m*	0.16	0.02
8*h*-9*i*	0.06	
8*i*-9*k*	0.35	
8*k*-9*l*	0.69	
Total 8-9	1.10	0.82
10*l*-12*m* plus 10*m*-12*n*	0.06	0.00

Cross sections for electron capture into specific n,l states σ_{nl} were derived from measured emission cross sections by means of a cascade code. A Gaussian distribution was used for the population of capture produced n states. Several l distributions were tested. The σ_{nl} were fitted to recover measured emission cross sections from upper levels populated either directly or indirectly by cascade. The fit is not very sensitive to l distribution. However, it seems that the $l=n-1$, $n-2$, and $n-3$ states are about equally populated by single-electron capture. Absolute cross sections for electron capture into $(n,l=n-1)$ states at 8- and 160-keV energies are given in Table III. From σ_{nl} (Table III) resulting from a fit to all measured emission cross sections at 160-keV energy, intensities of lines observed at 297.7, 297.6, and 297.4 nm were well reproduced (0.76, 0.22, and 0.06×10^{-14} cm^2 compared to 0.76, 0.28, and 0.05×10^{-14} cm^2 of Table II), confirming our assignment of these lines to 7*i*-8*k*, 7*h*-8*i*, and 7*g*-8*h* transitions, respectively (Table I). The same statement can be made for the 8*k*-9*l*, 8*i*-9*k*, and 8*h*-9*i* fitted and (measured) intensities 0.62(0.69), 0.23(0.35), and $0.08(0.06)\times10^{-14}$ cm^2.

TABLE III. Excitation cross sections for Ar VIII states populated by electron capture in Ar^{8+} impact on Cs.

Final state in Ar VIII		$\sigma_{excitation}$ (10^{-14} cm^2)	
n	l	160 keV	8 keV
8	7	0.07	0.02
9	8	0.20	0.21
10	9	0.23	0.21
11	10	0.15	0.02
12	11	0.05	0.00

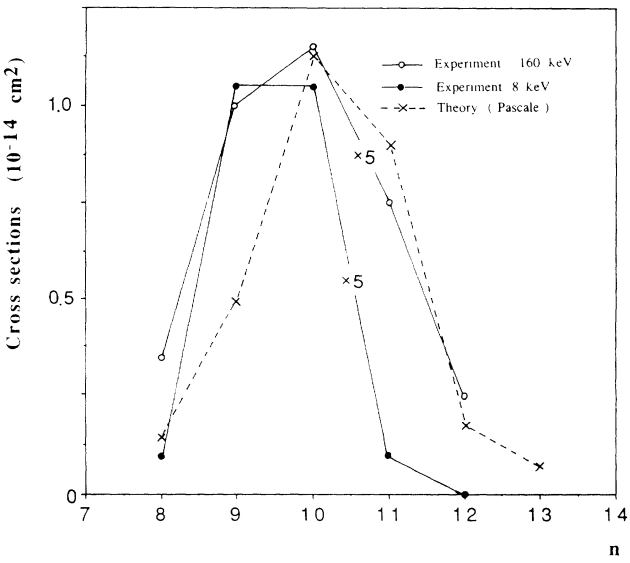

FIG. 4. Cross sections $\sigma_{n,l}$ for excited levels $8 \leq n \leq 13$ and $l = n-1$. $Ar^{8+} + Cs \rightarrow Ar^{7+}(n,l) + Cs^{+}$.

Measured capture cross sections into selected $(n, l = n-1)$ states are compared with theoretical results in Fig. 4. Calculated cross sections were obtained by Pascale, Olson, and Reinhold [9] using a three-body classical-trajectory Monte Carlo method with model potentials for $Ar^{8+} + Cs$ collisions at 80 keV. Present experimental data displayed in Fig. 4 were obtained at 8 and 160 keV. The CTMC n-distribution peaks at $n = 10$ and its width at half maximum is $\Delta n \simeq 2$.

Experimental n distribution also peaks at about $n = 10$ at 160-keV energy. At 8 keV it shifts to lower n values. Measured widths were $\Delta n \simeq 3$ at 160 keV and $\Delta n \simeq 2$ at 8 keV. These results can also be compared to estimations of the ECB model of Niehaus: $n_{max} = 10.4$, $\Delta n \sim 2$ at 160 keV, and $\Delta n \simeq 0.8$ at 8 keV. Thus experimental results were found to be in fair agreement with CTMC calculations and ECBM predictions of the n values which are predominantly populated after single-electron capture. However, measured absolute cross sections are lower than CTMC data by a factor of 5. Such discrepancies have also been found between the cross sections σ_n of CTMC and the distorted-wave approximation calculations when compared to the experimental values for $Au^{14+} + H_2$ at high energy [16] and between emission [17] cross sections and total capture cross section measured by the energy-gain method for similar collision systems at low energy [18].

IV. CONCLUSIONS

To summarize, collisions between slow Ar^{8+} and Ar^{9+} ions and cesium neutral atoms were studied using photon spectroscopy in the visible range. A few states with n values around $n_m = 10$ $(8 \leq n \leq 12)$ were populated by single-electron capture into Ar^{8+}. Lines observed between 250 and 470 nm were assigned to $\Delta n = 1$, 2, and 3 Rydberg transitions. l components of singly excited states and j components of core excited Rydberg states were resolved. Measured n distribution in Ar VIII after Ar^{8+} collisions in cesium were found in general agreement with ECBM and CTMC theoretical results. However, the measured cross sections are much lower than predictions of the CTMC method. More complete spectral analysis including the uv range and more precise determination of absolute cross section are still needed to know the nl distribution of the captured electrons, hence a challenge for more experimental and theoretical work in the future.

ACKNOWLEDGMENTS

This work was performed at LAGRIPPA (CEA-CNRS) at Grenoble. We want to thank T. Lamy, A. Brenac, and J. Lambolley for driving the argon beams at LAGRIPPA and G. Do Cao, A. Bourgey, and B. Terpend for skillful construction of experimental components.

[1] C. Harel and A. Salin, in *Electronic and Atomic Collisions,* edited by H. B. Gilbody *et al.* (Elsevier, Amsterdam, 1988), pp. 631–642.
[2] R. E. Olson, J. Phys. B **13**, 843 (1980).
[3] H. Ryufuku and T. Watanabe, Phys. Rev. A **20**, 1828 (1979).
[4] S. Martin, A. Denis, J. Désesquelles, and Y. Ouerdane, Phys. Rev. A **42**, 6564 (1990).
[5] M. Druetta, T. Bouchama, S. Martin, and J. Désesquelles, J. Phys. (Paris) Colloq. **49**, C1-365 (1988).
[6] S. Martin, G. Do Cao, A. Salmoun, T. Bouchama, A. Denis, J. Andrä, J. Désesquelles, and M. Druetta, Phys. Lett. A **133**, 239 (1988).
[7] S. Martin, A. Salmoun, Y. Ouerdane, M. Druetta, J. Désesquelles, and A. Denis, Phys. Rev. Lett. **62**, 2112 (1989).
[8] A. Niehaus, J. Phys. B **19**, 2925 91986).
[9] J. Pascale, R. E. Olson, and C. O. Reinhold, Phys. Rev. A **42**, 5305 (1990).
[10] J. P. Desclaux, Comput. Phys. Commun. **9**, 31 (1975).
[11] L. A. Bureeva and U. I. Safronova, Phys. Scr. **20**, 81 (1979).
[12] S. Bashkin, J. Bromander, J. A. Leavitt, and I. Martinson, Phys. Scr. **8**, 285 91973).
[13] J. O. Ekberg (private communication cited in [12]).
[14] M. Druetta, S. Martin, T. Bouchama, C. Harel, and H. Jouin, Phys. Rev. A **36**, 3071 (1987).
[15] A. Lindgard and S. E. Nielsen, At. Data Nucl. Data Tables **19**, 533 (1977).
[16] P. Hvelplund, E. Samsoe, L. H. Andersen, H. K. Haugen, and H. Knudsen, Phys. Scr. T3, 176 (1983).
[17] L. J. Lembo, K. Danzmann, Ch. Stoller, W. E. Meyerhof, and T. W. Hänsch, Phys. Rev. A **37**, 1141 (1988).
[18] W. Waggoner, C. L. Cocke, S. L. Varghese, and M. Stockli, Phys. Rev. A **29**, 2457 (1984).